The 8th Japan-Taiwan Conjoint Slide Conference

第八屆台日切片討論會

KYOTO

April 20-21, 2024

1. General information

Date: April 20-21, 2024

Venue: Inamori Hall, Shiran-kaikan, Kyoto University

President: 羽賀博典 Hironori Haga (Kyoto University)

Organizer: 南口早智子 Sachiko Minamiguchi (Kyoto University)

Contact information:

E-mail address: pathology@kuhp.kyoto-u.ac.jp

Mailing address: Department of Diagnostic Pathology, Kyoto University Hospital
54 Shogoin Kawahara-cho, Sakyo-ku, Kyoto 606-8507 Japan

2. Program at a glance

April 20th (Sat) - Kyoto City Tour and Welcome Reception

08:45	在京都八條都酒店大堂集合/都ホテル京都八条エントランス集合
09:00-17:30	京都觀光
18:00-20:00	歡迎會 (THE THOUSAND KYOTO)

April 21st (Sun) - Slide Conference and Poster Session

08:15	Meet at the entrance of Miyako hotel Kyoto Hachijo (Shuttle bus will take you to the venue)
08:30-09:00	Registration
09:00-09:10	Opening Ceremony
09:10-12:40	Slide conference (Inamori Hall)
10:25-11:05	Poster session (Hall Lobby)
12:40-14:00	Farewell Party (Yamauchi Hall)

3. Registration Fee for Taiwanese Participants

Please paid by Japanese Yen cash.

Participants joining the Kyoto City tour and Welcome Party, please make the payment at the Welcome Party reception on April 20th. For those not attending, please make the payment at the reception desk of the slide conference venue on the 21st.

Kyoto City tour	JPY 5,000
Welcome Reception	JPY 5,000
Slide Conference and Farewell Party	JPY 5,000

4. Access to the Venue

April 20th, 2024

Kyoto City Tour participants should meet at the entrance of the Miyako Hotel at **8:45 a.m.** After the tour, the bus will go directly to The Thousand Kyoto, the venue for the welcome reception.

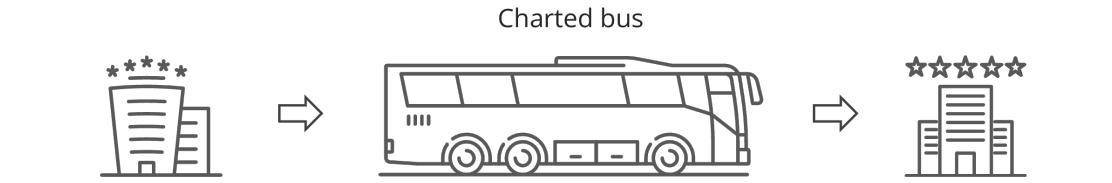

April 21st, 2024

A shuttle bus will run from the entrance of Miyako Hotel to Shiran-kaikan, and will leave at **8:15 a.m.** Please make sure to be on time.

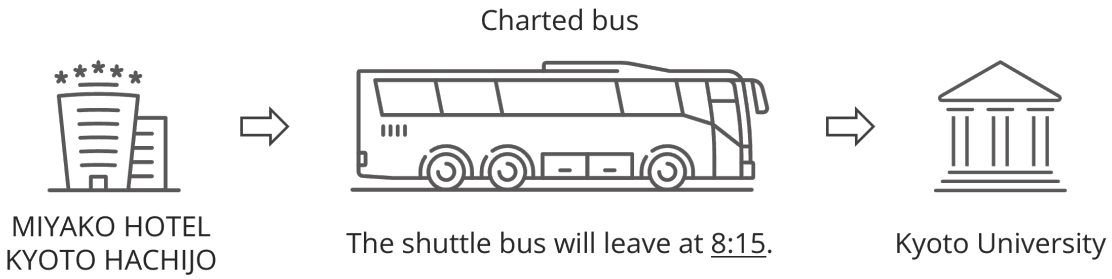

Linear bus service (HOOP, https://hoopbus.jp/) is available from Kyoto University to Kyoto Station Hachijo Exit. Please ask for a bus coupon if you wish to use it.

5. Venue Map

Ground floor, Shiran-kaikan

Please proceed to the second floor where staffs will guide you.

Second Floor, Shiran-kaikan

Reception is on the second floor.

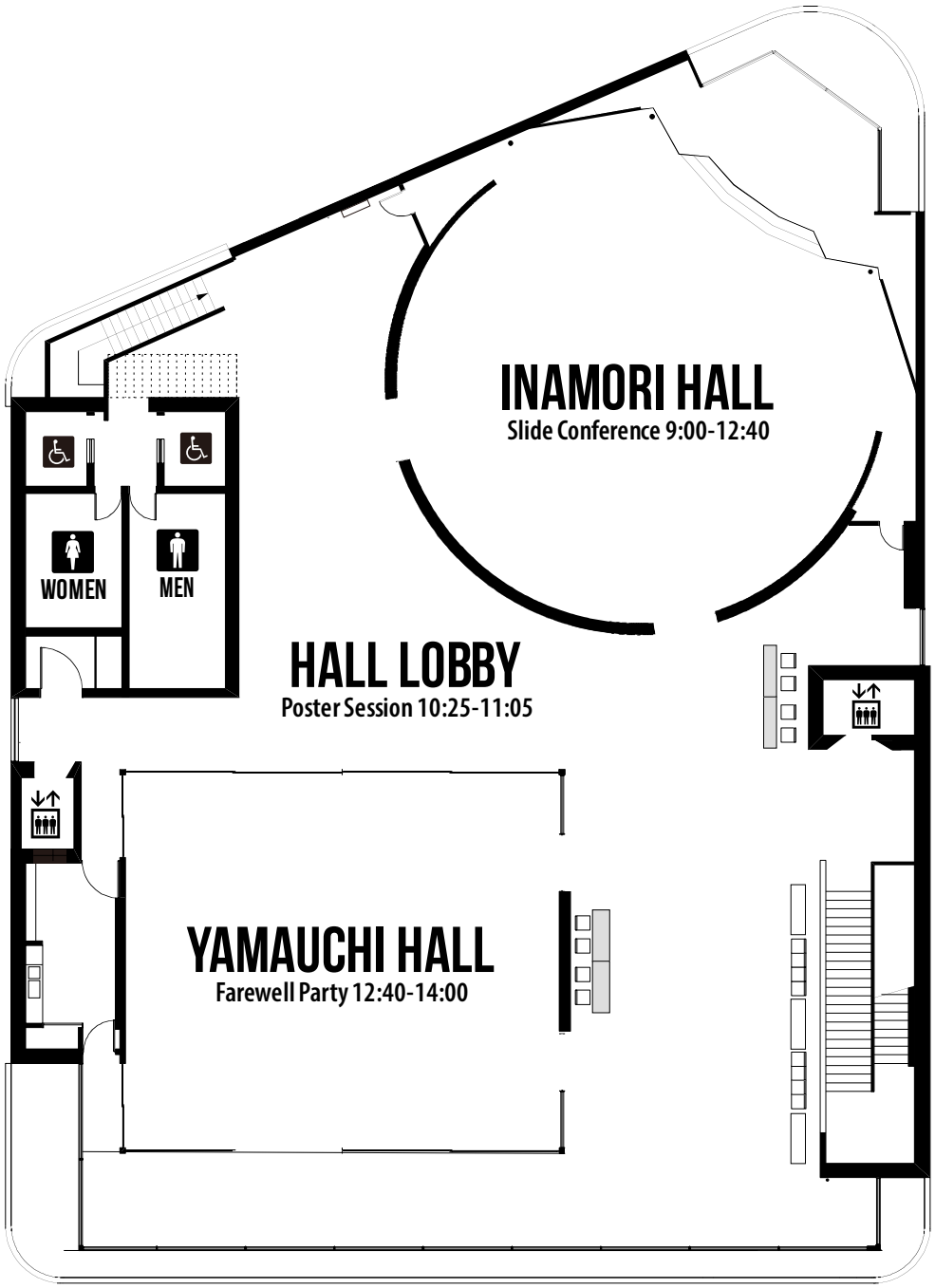

6. Virtual Slide Access

Japan cases (J-1~5)

https://pathology.kuhp.kyoto-u.ac.jp/

Username: jtcsc8

Password: jtcsc8

Taiwan cases (T-1~5)

https://tinyurl.com/jtcsc8

You can log in using any of the usernames provided below. However, please note that simultaneous logins with the same username are limited to 5 users. In case you encounter any errors, kindly try logging in with a different username.

Username:

twiap.guest01@guest.com
twiap.guest02@guest.com
twiap.guest03@guest.com
twiap.guest04@guest.com
twiap.guest05@guest.com

Password:

twiap_19670916

7. Instructions for Case Presenters

- Presentation time: 15 mins for each case (5 mins for discussant, 5 mins for submitter, 5 mins discussion)
- Presentation files should be created using Microsoft PowerPoint for PC. Functions of those made by Macintosh will not be secured.

8. Instructions for Poster Presenters

A display board giving a display area of approximately 90 cm (width) x 140 cm (height) will be provided for poster display. Pushpins will be provided to all poster presenters at the congress. Staff will be available to assist you. Please set up your poster between 08:30 - 08:55. In the poster session, there will be no moderator leading the session. It will be a free discussion involving posters.

Slide Conference Timetable

D: Discussant, S: Submitter, M: Moderator

08:30-09:00 Registration

09:00-09:10 Opening Ceremony

羽賀博典 Hironori Haga (Kyoto University)

鄭永銘 Yung-Ming Jeng (National Taiwan University)

09:10-09:25 Case 1 (T-1)

D 大江知里 Chisato Ohe (Osaka Metropolitan University)

S 林士堯 Shih-Yao Lin (Taipei Veterans General Hospital)

M 賴瓊如 Chiung-Ru Lai (Taipei Veterans General Hospital)

09:25-09:40 Case 2 (J-1)

D 胡家發 Chia-Fa Allen Hu (Kaohsiung Chang Gung Memorial Hospital)

S 間敬邦 Hirokuni Hazama (Kyushu University)

M 久岡正典 Masanori Hisaoka (University of Occupational and Environmental Health)

09:40-09:55 Case 3 (T-2)

D 長峯理子 Michiko Nagamine (National Cancer Center Hospital East)

S 李沛航 Pei-Hang Lee
(Kaohsiung Chang Gung Memorial Hospital and Chang Gung University College of Medicine)

M 黃玄贏 Hsuan-Ying Huang
(Kaohsiung Chang Gung Memorial Hospital and Chang Gung University College of Medicine)

09:55-10:10 Case 4 (J-2)

D 黃彥碩 Yen-Shuo Huang (Kaohsiung Medical University Hospital)

S 塩見達志 Tatsushi Shiomi (Kawasaki Medical School)

M 湊宏 Hiroshi Minato (Ishikawa Prefectural Central Hospital)

10:10-10:25 Case 5 (T-3)

D 大園一隆 Kazutaka Ozono (Kumamoto University Hospital)

S 許惠婷 Hui-Ting Hsu (China Medical University Hospital)

M 杭仁釩 Jen-Fan Hang（Taipei Veterans General Hospital)

10:25-11:05 Poster Session & Coffee Break

11:05-11:20 Case 6 (J-3)

D 張中亭 Sabrina Chang (Taipei Veterans General Hospital)

S 小野佐和子 Sawako Ono (Okayama University)

M 浦野誠 Makoto Urano (Fujita Health University Bantane Hospital)

11:20-11:35 Case 7 (T-4)

D 山下大祐 Daisuke Yamashita (Kobe City Medical Center General Hospital)

S 鄭子謙 Tzu-Chien Cheng (Keelung Chang Gung Memorial Hospital)

M 王任卿 Ren Ching Wang (China Medical University Hospital)

11:35-11:50 Case 8 (J-4)

D 張佳平 ChiaPing Chang (Taipei Veterans General Hospital)

S 都築豊徳 Toyonori Tsuzuki (Aichi Medical University)

M 牛久哲男 Tetsuo Ushiku (University of Tokyo)

11:50-12:05 Case 9 (T-5)

D 合田直樹 Naoki Goda (Kyoto University)

S 陳琬清 Wan-Ching Chen (Taichung Veterans General hospital)

M 鄭永銘 Yung-Ming Jeng (National Taiwan University)

12:05-12:20 Case 10 (J-5)

D 黃中彥 Chung-Yen Huang (National Taiwan University Hospital)

S 寺本祐記 Yuki Teramoto (Kyoto University Hospital)

M 松原修 Osamu Matsubara (Hiratsuka Kyosai Hospital)

12:20-12:40 Closing Ceremony

鄭永銘 Yung-Ming Jeng (National Taiwan University)

小田義直 Yoshinao Oda (Kyushu University)

Case 1 (T-1)

Submitter: 林士堯 Shih-Yao Lin
Institution: Taipei Veterans General Hospital
Case Subspecialty: Gynecology Pathology
Location and Specimen Type: Retroperitoneum, Tumor excision
Short History:
This is a 54-year-old female diagnosed with leiomyosarcoma after myomectomy in another hospital on 2021/11/1. Staging surgery was suggested at that time, and she decided to transfer to our hospital. Our gynecologist performed total hysterectomy with bilateral salpingo-oophorectomy and bilateral pelvic lymph node dissection for her on 2021/12/17. Pathological examination revealed quite scant atypical cells in the uterus and no other involvement. She was free of disease until 2023/6/10 when lower abdomen MRI revealed a newly developed 7.4 cm retroperitoneal tumor in the cul-de-sac close to the rectum. She received tumor excision with low anterior resection on 2023/6/21.

Case 2 (J-1)

Submitter: 間敬邦 Hirokuni Hazama
Institution: Department of Anatomic Pathology, Graduate School of Medical Sciences, Kyushu University
Case Subspecialty: Bone and soft tissue
Location and Specimen Type: Sacrum, open biopsy and resection
Short History:
74 years old, Male
The patient with no medical history experienced progressively worsening sacral pain in the supine position for one year. On physical examination, an elastic-soft mass was detected at the sacral region. The patient had no bladder and bowel dysfunction. Plain X-ray-images showed focal osteosclerosis and cortical disruption of the coccyx suggesting osteolysis on the lateral view. Plain CT-images showed a well-defined mass, about 11cm in size, with calcification and contiguous to the sacrococcygeal bone. MRI-images revealed internally heterogeneous low- to equivalent-signal on T1-weighted images and high-signal on T2-weighted images. PET-CT-images showed no obvious systemic metastasis. Open biopsy was performed. Histologically, the specimen showed a sheet-like proliferation of atypical cells having clear to eosinophilic cytoplasm, accompanied by myxoid matrix and hemorrhage. Immunohistochemically, the atypical cells were positive for brachyury. These features indicated that of conventional chordoma. After the biopsy, wide resection was performed on the tumor. Grossly, the mass was a yellowish-white, well-defined lesion with hemorrhage and necrosis.

Case 3 (T-2)

Submitter: 李沛航 Pei-Hang Lee, MD
Institution: Department of Anatomical Pathology, Kaohsiung Chang Gung Memorial Hospital and Chang Gung University College of Medicine
Case Subspecialty: Bone and soft tissue
Location and Specimen Type: Lung, right lower lobe, wedge resection
Short History:
This is a 33-year-old man who, a non-smoker, denied any relevant systematic disease. During health check-up in August 2023, chest radiography revealed a solitary right lower lung nodule, which was further demonstrated to be spiculated by chest computed tomography, raising suspicions of malignancy. Wedge resection was performed in September 15th, 2023. The specimen submitted consists of a wedge resection of the right lower lung, measuring 4.9 x 4.6 x 1.8 cm and weighing 10.5 gm. The pleural surface showed focal retraction. On cutting, the ill-defined tumor, measuring 1.3 x 1.2 x 1.1 cm, was located beneath the pleura, 0.6 cm from the parenchymal resection margin, and grayish-white and solid in appearance.

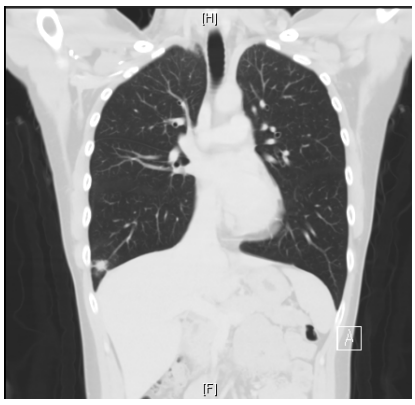

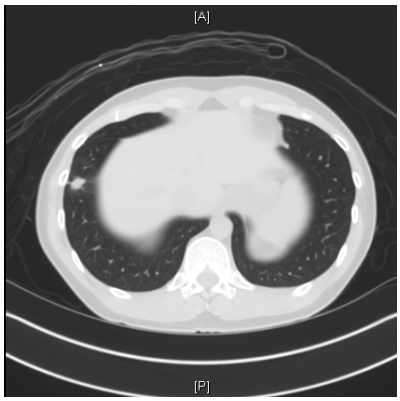


Case 4 (J-2)

Submitter: 塩見達志 Tatsushi Shiomi, Hirotake Nishimura, Takuya Moriya
Institution: Department of Pathology, Kawasaki Medical School
Case Subspecialty: Hematology
Location and Specimen Type: Dura mater
Short History:
A case of foam cells distributed in the dura mater
A 59-year-old Japanese man presented with gait disturbance and dysarthria. His family history was not significant. Magnetic resonance imaging revealed thickening of the dura mater in the cerebrum. Laboratory testing showed elevated serum concentrations of sIL-2 receptor (2751 U/mL; normal range, 122-496 U/mL), IgG (2014 mg/dL; normal range, 870-1700 mg/dL), and IL-6 (78.1 pg/mL; normal range, 0-8 pg/mL). A biopsy of the dura mater revealed distributed foam cells with lymphocytes and plasma cells. Immunohistochemically, these foam cells were positive for CD68 (PGM1), CD163, and fascin.

Case 5 (T-3)

Submitter: 許惠婷 Hui-Ting Hsu
Institution: China Medical University Hospital
Case Subspecialty: Head and neck
Location and Specimen Type: Nasal cavity, maxillectomy
Short History:
A 56-year-old woman, with a history of hypertension, presented with intermittent right nasal bleeding for 8 months. During the nasendoscopy examination, the presence of blood over the sinus ostium was noted. The head and neck CT scan of the paranasal sinuses demonstrated a 30x28x25 mm lesion in the right maxillary and ethmoid sinuses, with destruction of right nasal turbinate and right inferior orbital wall, and bulging into right inferior orbit. Subsequently, a maxillectomy and repair of the orbital floor were performed.

Case 6 (J-3) - A case of parotid gland tumor

Submitter: 小野佐和子 Sawako Ono[1], Hidetaka Yamamoto[1], Kenji Nishida[2]
Institution:
1. Department of Pathology and Oncology, Graduate School of Medicine, Dentistry and Pharmaceutical Sciences, Okayama University
2. Department of Pathology, Okayama University Hospital
Case Subspeciality: Head and neck
Location and Specimen Type: Parotid gland, parotidectomy
Short History:
54 years, Male
A patient presented with a several-year history of a right parotid mass. Magnetic resonance imaging (MRI) revealed a 3.5-cm nodular mass in the right parotid gland and Warthin tumor was suspected. The positron emission tomography-computed tomography (PET-CT) detected no other primary or metastatic lesions. The patient underwent parotidectomy. Macroscopically, the resected specimen showed a solid well-defined mass with uniform color tone.

Case 7 (T-4)

Submitter: 鄭子謙　Tzu-Chien Cheng
Institution: Keelung Chang Gung Memorial Hospital
Case Subspecialty: Hematolymphoid
Location and Specimen Type: Posterior aspect of right-sided upper gingiva, and edentulous ridge of maxilla (#15 and #16 area), wide excision including inferior maxillectomy

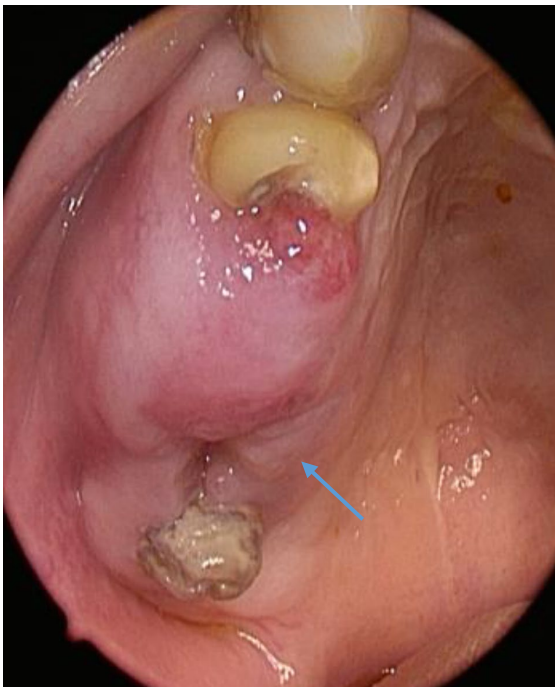

Fig. 1 Clinical intraoral finding

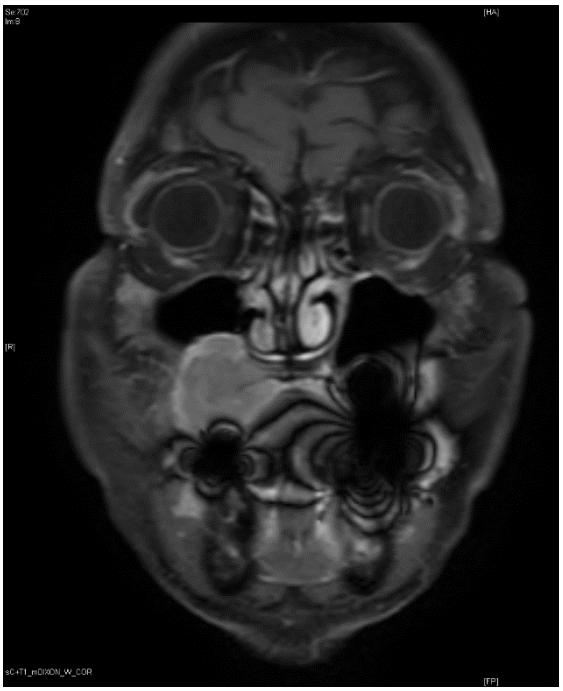

Fig. 2 Coronal MRI image, T1WI with contrast enhanced

Short History:
The 74-year-old man presented with a progressively enlarging ulcer on the right upper gingiva, accompanied with pain for months (Fig. 1). The patient reported no significant past medical history, personal history, or family history. Upon physical examination, an ulcerative lesion was observed on the posterior aspect of right-sided upper gingiva. No palpable neck lymphadenopathy was noted.

Laboratory tests revealed mild normocytic anemia (Hb = 11.3 g/dL, HCT = 33.2%, MCV = 95.4 fL) and leukopenia (WBC = 3,500 per μL). The platelet count (PLT = 186,000 per μL)

was normal.

Both CT scan and MRI of the head and neck region demonstrated a tumor measuring up to 3.4 cm in diameter on the floor of the right maxillary sinus, with bone destruction (Fig. 2). A subsequent PET scan identified a tumor in the right-sided upper gingiva (a standardized uptake value (SUV) of 5.7, score 4) and a right-sided paratracheal nodal lesion (score 2).

A wide excision including inferior maxillectomy and right-sided neck dissection (level I to level III) were performed. Gross examination of the excised tissue revealed an infiltrative white tumor measuring 2.8 x 2.5 x 2.2 cm, with invasion into the maxilla. Histologically, all the dissected lymph nodes were free of malignancy.

A panel of immunohistochemical stains was performed. The tumor cells showed patchy staining with INSM1 and synaptophysin, and were negative for PanCK (AE1/AE3), CAM5.2, p40, NUT, chromogranin, SOX10, S100, HMB45, CD99, NKX 2.2, desmin, CD45 (LCA), CD3, and CD20, along with intact INI1 and BRG1 nuclear expression.

Case 8 (J-4) - A case of Unknown Primary Cancer (CUP)

Submitter: 都築豊徳 Toyonori Tsuzuki
Institution: Department of Surgical Pathology, Aichi Medical University, School of Medicine
Case Subspecialty: Genitourinary Pathology
Location and Specimen Type: Lymph node, excisional biopsy
Short History:
73 years, Male
A patient was referred to the Department of Hematology in our hospital due to left leg swelling and enlarged lymph nodes in the groin. The patient's blood tests showed that their CEA level was 6.9 ng/mL (normal range: <5.0ng/mL), PSA level was 5.5 ng/mL (normal range: <5.0ng/mL), and soluble IL-2R level was 899 U/ml (normal range: 121-613 U/ml). No hematological disorders were detected. An inguinal lymph node biopsy was performed, which revealed that the lymph node was effaced by cancerous cells that were positive for CK7 and PSA, and negative for CK20, CDX-2, and PAX8. Even though CT, MRI, and PET/CT scans were performed, no abnormal image findings were detected. The patient underwent a prostate needle biopsy, gastroscopy, and colonoscopy three months later, but no abnormal findings were found.

Case 9 (T-5)

Submitter: 陳琬清 Wan-Ching Chen
Institution: Taichung Veterans General hospital.
Case Subspecialty: Head and Neck.
Location and Specimen Type: Nasal, paranasal, and skull base tumors
Short History:
The 72-year-old female patient had no reported medical history. She presented to the hospital this time due to recent issues with her eyes being unable to focus.
Upon examination, only nasal congestion was observed, and serology tests yielded normal results. An MRI from another hospital revealed a substantial brain tumor (6.5 cm) over the frontal base with downward extension and nasal cavity invasion. Suspected to be an atypical meningioma, she was referred to our hospital for further evaluation and surgical intervention.
During the surgery, a frozen sample was sent for analysis, and the initial impression from the surgeon was atypical meningioma. Our initial frozen assessment indicated a meningioma with atypical features. Subsequently, the patient underwent trans-sphenoidal tumor removal.

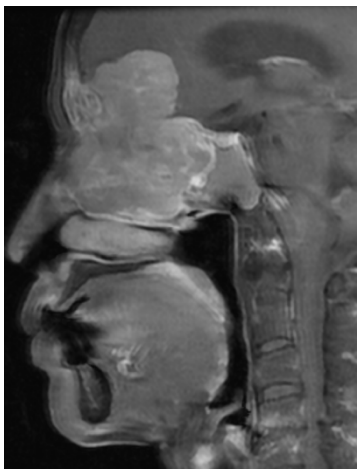
MRI: T1 sagittal view

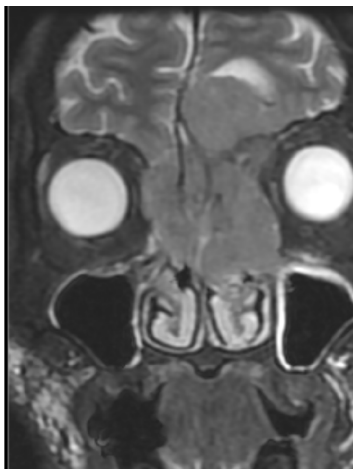
MRI: T2 coronal view

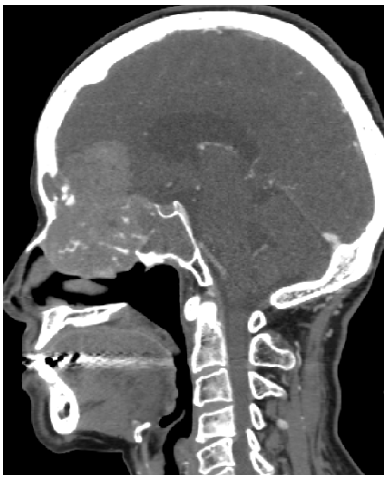
CT with contrast

Case 10 (J-5)

Submitter: 寺本祐記 Yuki Teramoto
Institution: Department of Diagnostic Pathology, Kyoto University Hospital
Case Subspecialty: Pulmonary Pathology
Location and Specimen Type: Lung, left upper lobe, lobectomy.
Short History:
The patient was a 70-year-old male with no smoking or family history.
6 years prior to surgery: Prostate biopsy revealed acinar adenocarcinoma with Gleason score (GS) 3+3, which was followed up.
4 years prior to surgery: Re-biopsy upgraded the prostate cancer to GS 4+4, and the patient underwent hormone therapy and IMRT. Since then, PSA remained at 0.6~1.1 ng/ml and was considered to be under good local control.
Year of surgery: A 4.4 cm-sized mass was found in the left upper lobe of the lung on chest X-ray, and the patient underwent left upper lobectomy at our hospital. The pathological diagnosis was initially “colloid adenocarcinoma of the lung”. However, the thoracic surgeon pointed out that the patient had a history of prostate cancer and added NKX3.1 immunostaining, which was diffusely positive for tumor cells. Therefore, the pathological diagnosis was corrected as "metastatic carcinoma of prostatic origin”.
1 year after surgery: Sudden cognitive decline and disorientation appeared. A CT scan of the head indicated the appearance of multiple brain tumors. Based on the clinical history, it was assumed to be metastasis of prostate cancer. However, because the course deviated from the common clinical course of prostate cancer, the urologist asked the GU pathologist to reexamine the histology of the lung tumor.

Poster 1 (P-1)

Cardiac pseudomyogenic hemangioendothelioma with a novel *MAPK1IP1L::FOSB* fusion: A case report.

張珍 Chen Chang[1], Nai-Syuan Chen[1], Wan-Shan Li[2], Yu-Chien Kao[1]

1. Department of Pathology, National Cheng Kung University Hospital, College of Medicine, National Cheng Kung University, Tainan, Taiwan
2. Division of Molecular Pathology, Department of Pathology, Chi Mei Medical Center, Tainan, Taiwan

Pseudomyogenic hemangioendothelioma (PHE) is a rare, intermediate-grade vascular tumor with histological features mimicking myoid tumors or epithelioid sarcomas. Predominantly affecting young adults under 40 years of age, PHE often presents as multiple discontiguous nodules in different tissue planes from cutaneous, subcutanoeus to intramuscular and intraosseous sites. The most common location is the lower limbs (55%), followed by upper limbs (20%), trunk (20%) and rarely over the head or neck. The tumor is driven by FOSB overexpression and characterized by FOSB gene rearrangement. We report a case of a 4-year-old girl who presented with syncope, intermittent pallor, weakness, and fever. An echocardiogram and CT scan revealed a large heart tumor in the right atrium (RA) and right ventricle. The patient underwent tumor excision, revealing a 5.2x2.5cm tumor originating from the RA wall near the atrioventricular groove. Histopathological examination showed infiltrative spindle cell proliferation within a myxoid stromal background. The tumor cells had mild nuclear irregularity and occasional elongated eosinophilic cytoplasm, arranged in loose fascicles or haphazardly dispersed in the myxoid stroma. In addition, foci of epithelioid cells with eosinophilic cytoplasm were also present. Lymphocytic infiltration, intratumoral hemorrhage, and many delicate capillaries were also seen in areas. Immunohistochemically, the tumor cells were positive for ERG, AE1/AE3, FOSB, focally positive for CD34 and SMA, and negative for CD31, S100, ALK (5A4), ROS-1, desmin, myogenin, MDM2, CDK4, Pan-TRK, and calretinin. Targeted RNA sequencing (Archer FusionPlex Pan-Solid v2 panel) identified a novel *MAPK1IP1L::FOSB* fusion, supporting the diagnosis of PHE. In conclusion, this case underscores the diagnostic challenges associated with PHE and the need for comprehensive histopathological and molecular analysis for accurate diagnosis. The unusual presenting age and location also pose diagnostic difficulties.

Poster 2 (P-2)

Melanotic Xp11 Translocation renal cancer / PEComa: A Case Report

陳怡儒 I-JU CHEN
Department of Pathology, Wan Fang Hospital, Taipei Medical University, Taipei, Taiwan

Melanotic Xp11 translocation renal cancer is a rare renal neoplasm, with approximately 20 cases documented in the literature so far. Since this type of tumor exhibits similar clinical characteristics, morphology and immunoprofile with perivascular epithelioid cell tumor (PEComa), some studies have considered it as a variant of Xp11 translocation PEComa.[1] Herein, we report a case of a 30-year-old female with right renal tumor. Her past medical history included focal endometrial hyperplasia without atypia. She presented to our outpatient department due to incidental finding of a right renal tumor in the health exam. Magnetic resonance imaging showed a 5.7 cm mass lesion at right kidney, with hemorrhagic part, but no obvious fat component. Therefore, a laparoscopic right radical nephrectomy was performed. Grossly, there was a well-circumscribed and black tumor, measuring 5.3 x 4.8 x 4.8 cm in size, in the lower pole of the kidney. Microscopically, it showed a well-demarcated tumor, arranged mainly in solid nested pattern. The tumor cells revealed epithelioid morphology, abundant clear to eosinophilic granular cytoplasm with heavy melanin pigments, and round nuclei with occasional nucleoli. No tumor necrosis, no atypical mitotic figure, and no pleomorphism was found in the specimen. Lymphovascular invasion was observed. Melanin pigments were demonstrated by Fontana-Masson special stain. Immunohistochemically, the tumor cells were immunoreactive to TFE3, focally positive to HMB45, while negative for PAX8, Melan-A, SOX10, and S100. Ki-67 proliferative index was 1-2%. According to the morphology and immunohistochemical studies, melanotic Xp11 translocation renal cancer / PEComa was diagnosed. Due to its large size (> 5 cm), uncertain malignant potential was indicated.[2]

The differential diagnosis may include classic angiomyolipoma (AML) / PEComa, melanoma, and TFE3-rearranged renal cell carcinoma. The abundant melanin pigment and immunoreactivity to HMB45 may arouse worries about melanoma. However, primary melanoma arising from kidney is rare. Negativity for SOX10 and S100, and positivity for TFE3 rule out the diagnosis of melanoma. Also, negativity for PAX8 can rule out the TFE3-

rearranged renal cell carcinoma. Xp11 translocation PEComa is different from classic AML / PEComa of the kidney in the various aspects. The population of patients of the former are young and female predominant, and the clinical behavior is more aggressive. They almost have an exclusively epithelioid clear cell morphology, while both classic AML and epithelioid AML may show component of spindle cell morphology. Immunohistochemically, Xp11 translocation PEComa shows minimal to absent immunoreactivity for muscle markers. TSC1 or TSC2 genes alteration, or a clinical association with tuberous sclerosis are not seen.[3,4] According to the literature, tumor size >5 cm, infiltrative growth pattern, high nuclear grade, necrosis, and mitotic activity >1/50 HPF are associated with subsequent aggressive clinical behavior.[2]

Reference:

1. Argani Pedram et al. (2016) TFE3-Fusion Variant Analysis Defines Specific Clinicopathologic Associations Among Xp11 Translocation Cancers. Am J Surg Pathol, 40(6):723–737.
2. Folpe, Andrew L, et al. (2005) Perivascular Epithelioid Cell Neoplasms of Soft Tissue and Gynecologic Origin A Clinicopathologic Study of 26 Cases and Review of the Literature. Am J Surg Pathol, 29(12): p 1558-1575
3. Holger Moch, et al. TFE3-rearranged renal cell carcinomas. In: WHO Classification of Tumours Editorial Board. Urinary and male genital tumours [Internet]. Lyon (France): International Agency for Research on Cancer; 2022 [cited 2024 Feb 16]. (WHO classification of tumours series, 5th ed.; vol. 8). Available from: https://tumourclassification.iarc.who.int/chaptercontent/36/25
4. Epithelioid angiomyolipoma / epithelioid PEComa of the kidney. In: WHO Classification of Tumours Editorial Board. Urinary and male genital tumours [Internet]. Lyon (France): International Agency for Research on Cancer; 2022 [cited 2024 Feb 16]. (WHO classification of tumours series, 5th ed.; vol. 8). Available from: https://tumourclassification.iarc.who.int/chaptercontent/36/33

Poster 3 (P-3)

A case of spermatocytic tumor

松浦悠実 Yumi Matsuura, Shintaro Takahashi, Yasuto Fujimoto, Yuka Mikami, Hirotake Nishimura, Takuya Moriya
Kawasaki Medical School

A man in his 50s consulted a urologist due to a mass in his right testicle. Contrast-enhanced magnetic resonance imaging revealed a round mass approximately 23 mm in diameter, showing homogeneous contrast and diffusion restriction. Blood tests showed human chorionic gonadotropin (HCG) <2.3 mIU/mL, alpha-fetoprotein (AFP) 3.5 ng/mL, and lactate dehydrogenase (LDH) 157 U/L, prompting suspicion of a seminoma, leading to a high orchiectomy.
Upon gross examination, a well-defined white-toned mass was observed in the testis. Histologically, the tumor exhibited three types of round tumor cells of varying sizes, with the nuclear chromatin of intermediate and giant cells appearing granular or filamentous patterns. Mitotic figures, including atypical forms, were scattered, with minimal lymphocytic infiltrates. The presence of germ cell neoplasia in situ (GCNIS) remained uncertain. Immunohistochemistry revealed SALL4 positivity in tumor cells, partial weak positivity for c-KIT, and negativity for OCT-3/4 and D2-40 with no GCNIS detected. Consequently, a diagnosis of spermatocytic tumor was established.
Spermatocytic tumors, classified as GCNIS-unrelated germ cell tumors by the World Health Organization, are rare, constituting approximately 1% of testicular germ cell tumors. While microscopically similar to seminomas, they differ in the described characteristics. Given their typically benign course, it is important to differentiate them from seminomas, which have distinct prognoses. Accurate diagnosis depends on disease recognition and careful observation of HE staining, supplemented by the active use of immunohistochemistry for assistance.

Poster 4 (P-4)

A case of gastric lipoma mimicking well differentiated liposarcoma

藤本康人 Yasuto Fujimoto, Syunsuke Yorifuji, Seiya Kinoshita, Tatsushi Shiomi and Takuya Moriya
Kawasaki Medical School

A patient is a 45-year-old woman. She presented with shortness of breath on exertion and melena from a week ago, and visited our emergency room. Blood tests revealed iron deficiency anemia, and contrast-enhanced computed tomography (CT) showed no obvious extravasation, but a ruptured gastric submucosal tumor (SMT) was suspected. Endoscopy exhibited a snowman-shaped SMT over 50 mm in size extending from gastric angle to greater curvature of antrum. Endoscopic ultrasonography (EUS) showed a homogenous hyperechoic tumor contiguous with the submucosa. Contrast-enhanced magnetic resonance imaging (MRI) revealed a tumor composed of fatty components, with no internal enhancing components, and was considered to be a lipoma clinically. An endoscopic biopsy specimen from the tumor showed a fatty stromal component, with some cells that appeared atypical histopathologically. The tumor was considered to have adipose differentiation, but it was difficult to determine whether it was benign or malignant. A pyloric gastrectomy was performed for diagnostic and therapeutic purposes. The surgical specimen microscopically showed a tumor composed mainly of mature adipose tissue, accompanied by an intervening component of spindle-shaped stromal cells proliferating with collagen fibers. The adipocytes of variable size and atypical-looking nuclear enlargement of adipocytes and stromal cells were identified. Inflammatory cell infiltration was also seen in some areas. Immunohistochemically, MDM2 focal weakly-positive, CDK4 focal weakly-positive, p16 focal positive, CD34 positive (stromal cells), and Rb positive (retained expression). No significant increase in Ki-67 (MIB-1) labeling index was observed. In addition, FISH performed at that facility showed no amplification of the MDM gene. Based on these fingdings, a diagnosis of lipoma (atypical) was made, with a well differentiated liposarcoma being ruled out. The postoperative course is uneventful, and no recurrence. Although gastric lipomas are rare benign tumor (accounting for only 5% of all gastrointestinal primary lipomas and less than 1% of gastric tumors), the

histological diagnosis is usually straight forward. We report the case of lipoma with atypia in which we had difficulty in differentiating from well differentiated liposarcoma.

Poster 5 (P-5)

An autopsy case of a patient with myotonic dystrophy

古味和晃 Kazuhiro Komi, Hirotake Nishimura, Yukari Nagasaki, Takayuki Konishi and Takuya Moriya
Kawasaki Medical School

Here we present an autopsy case of a 60-year-old woman with a history of myotonic dystrophy (DM1) lasting approximately 45 years. Clinically, she presented with gait disturbance, hachet face, and grip myotonia, while genetic testing revealed prolonged CTG repeats (1000 repeats). At autopsy, the patient's fixed brain weight was 1090 g. Atrophy of the gross frontal lobe and parahippocampal gyrus was observed, while neurofibrillary tangles were histologically observed in the parahippocampal gyrus. Immunostaining for anti-phosphorylated tau (AT8) revealed positive findings from the limbic system to the lower temporal lobe (AT8 stage III), with no positive findings for amyloid beta. Although the pathological findings were consistent with primary age-related tauopathy, tau pathology was observed not only in the limbic system, but also extensively in the brainstem and spinal cord. Plaque-like structures were observed in the midbrain tegmentum. Furthermore, positive findings were observed in gray matter neurons and neurites in the spinal cord. No alpha-synuclein pathology or positive findings for pTDP-43 were observed. Nuclei in the skeletal muscle were arranged in a chain-like pattern. Other organs exhibited mild pneumonia, fatty degeneration of hepatocytes, pancreatic cysts, and adenomatous goiters. However, no significant morphological changes were observed in the endocrine organs.
DM1 is a systemic disease well-known among medical students in Japan. However, autopsy pathology can pose a challenge for pathologists as it requires deep knowledge of central nervous system and muscle pathology.

Poster 6 (P-6)

Conventional spindly malignant peripheral nerve sheath tumor arising from a schwannoma with *SH3PXD2A*::*HTRA1* fusion

李致豪 Chih-Hao Li, Hsuan-Ying Huang
Department of Anatomic Pathology, Kaohsiung Chang Gung Memorial Hospital, Kaohsiung, Taiwan

Schwannomas are common benign peripheral nerve sheath tumors, consisting nearly purely of neoplastic schwannian cells. At the molecular level, *NF2* inactivating mutation represents the crucial genetic alteration in up to 75% of sporadic schwannomas. Recently, a fusion between the *SH3PXD2A* and *HTRA1* genes is proposed as an alternative tumorigenic mechanism, present in approximately 10% of cases, and significantly associated with a “serpentine palisading” histological pattern. Malignant transformation of schwannomas is scarce and, once occurring, mostly takes the form of epithelioid malignant peripheral nerve sheath tumor (MPNST), with the occurrence of conventional spindly MPNST being ultrarare in schwannomas. Herein, we describe a spindly MPNST associated with a schwannoma harboring *SH3PXD2A*::*HTRA1* fusion, manifesting as a pre-sacral mass in a 56-year-old female. The patient had a left breast cancer (invasive carcinoma of no special type) post treatment in 2019. She presented with soreness over lower back in October 2021. Computerized tomography (CT) scans revealed a 9 cm tumor at pre-sacral region, for which surgical excision was performed. Histologically, there were juxtaposed hypercellular and hypocellular components, with compact fascicles of hyperchromatic spindle cells with frequent mitoses in the former. The hypocellular component showed plump to oval cells arranged in a distinctive “serpentine palisading” pattern with bland-appearing cytology without mitosis. Immunohistochemically, SOX10 reactivity is focal and patchy in the MPNST area but diffuse in the schwannomatous component, while the expression of both H3K27me3 and INI1 is retained in both components. Furthermore, a fusion between *SH3PXD2A* (exon 6) and *HTRA1* (exon 2) was detected in both components by RT-PCR with confirmatory Sanger sequencing and BaseScope RNA in situ hybridization, hence arriving at the diagnosis of spindly MPNST arising from a fusion-positive schwannoma. The patient received adjuvant radiotherapy (60 Gy in 30 fractions) because of positive surgical margins, while local recurrence was noted in May 2022. According to follow-up

imaging studies, this patient developed widespread metastases to the lung, liver, and bone and expired in January 2023. Spindly MPNST arising in a schwannoma is ultrarare. Recognizing the “serpentine palisading” histological pattern in the schwannomatous component is helpful to guide the potential cases for molecular detection of the *SH3PXD2A*::*HTRA1* fusion.

Poster 7 (P-7)

Cytoplasmic lipid droplets and adipophilin expression correlate with poor prognosis in diffuse large B-cell lymphoma

王淑嫻 Shu-Hsien Wang, MD, and Kung-Chao Chang, MD, PhD*

Department of Pathology, National Cheng Kung University Hospital, College of Medicine, National Cheng Kung University, Tainan, Taiwan
* Correspondence:
Kung-Chao Chang, MD, PhD, Department of Pathology, National Cheng Kung University Hospital, College of Medicine, National Cheng Kung University, 138 Sheng-Li Road, Tainan, 704 Taiwan. Tel.: +886-6-235-3535 ext. 2636; Fax: +886-6-276-6195; E-mail: changkc@mail.ncku.edu.tw

Burkitt lymphoma, a neoplasm with the highly rapid turnover, is characterized by cytoplasmic vacuoles, which are best revealed by vital staining smears. The cytoplasmic vacuoles have been demonstrated to be lipid droplets (LDs), which are decorated by perilipin 2 (adipophilin). The phenomenon of cytoplasmic vacuoles (LDs) is universal and thus plays no role in prognosis of patients with Burkitt lymphoma. In contrast, cytoplasmic vacuoles (LDs) seem not to be a ubiquitous feature in diffuse large B-cell lymphoma (DLBCL) and their role in clinicopathologic characters of DLBCL patients would be intriguing. DLBCL is the most common type of malignant lymphoma and its molecular classification carries prognostic significance and therapeutic implication, including one type characterized by metabolic reprogramming with enhanced lipogenesis, which is reflected by cytoplasmic LDs and represented by cytoplasmic vacuoles in cytology smears. We, thus, aimed to test the role of lipid biogenesis in clinicopathologic features of DLBCL patients. The study cohorts were composed of three groups: 1) DLBCL patients with lymphomatous effusional cytology smears available (n=52); 2) DLBCL cases with imprint cytology smear available on frozen sections during intraoperative consultation (n=32); and 3) DLBCL cases with solid lymphoma tissues for adipophilin immunostaining (n=85). The cytology smears were reviewed by two pathologists and percentage of tumor cells among all nucleated cells and percentage of tumor cells with LDs were evaluated by oil immersion at 10 fields. For selected cases, flow cytometry and/or cell blocks with

immunohistochemical staining were performed to validate tumor involvement. We first validated cytoplasmic vacuoles to be lipid droplets by Oil-red-O stain, fluorescent Bodipy stain and electron microscopy examination. Then, we found that the phenomenon of cytoplasmic vacuoles in DLBCL cells was present more frequently in effusion specimens than in solid tumor imprinting specimens (32.7% [17/52] vs. 9.4% [3/32], p=0.015, Fisher exact test). Since DLBCL with lymphomatous effusion was a poor prognosticator than those without, even worse than stage IV disease (Am J Clin Pathol 2015;143(5):707-15), it indicates that lymphoma cells in effusions may represent a more aggressive biology behavior than those in solid tumors, as presented with many cytoplasmic LDs, that is, enhanced lipogenesis. In addition, DLBCL patients (n=52) with LDs in effusional lymphoma cells carried a worse prognosis (p=0.029, log-rank test), had a higher International Prognostic Index (IPI) score (94% vs. 66%, p=0.026), and showed a trend for higher LDH serum levels (>225 IU/L, 100% vs. 82%, p=0.065) and high-stage disease (stages III-IV; 100% vs. 80%, p=0.060) than those without LDs in effusional lymphoma cells. Moreover, using adipophilin as a surrogate marker for the presence of LDs, we found that in another cohort of DLBCL (n=85), expression of adipophilin in solid tumor cells predicted a poorer prognosis than those without adipophilin expression (p=0.007, log-rank test), correlated with a higher IPI score (63% vs. 30%, p=0.005), and showed a trend for higher LDH levels (79% vs. 58%, p=0.073). To the best of our knowledge, we are the first to show that presence of LDs predict poorer prognosis in DLBCL patients with lymphomatous effusions and expression of adipophilin predicts poorer prognosis in patients with solid DLBCL. Our findings, therefore, highlight the role of LDs and adipophilin expression in prognostic prediction in patients with DLBCL and suggest that cytologic examination of lymphomatous effusions with LDs should be routinely performed for prognostic and therapeutic stratification.

Poster 8 (P-8)

A case of pulmonary metastasis with interstitial spread of sinonasal adenoid cystic carcinoma

松野岳志 Takeshi Matsuno, Takae Inayoshi, Hironori Miyake, Takashi Matsutani, Hirotake Nishimura, Tatsushi Shiomi, Takuya Moriya
Kawasaki medical school

A 64-year-old woman was diagnosed with sinonasal adenoid cystic carcinoma (cT4N0M0, cStage IVB) and underwent induction chemotherapy and proton beam therapy. 4 years later, the first local recurrence was detected. At the same time, Computerized tomography (CT) revealed a partial solid ground glass nodule (24mm in size) in the right upper lobe. As this lesion was suspected to be primary lung adenocarcinoma, a wedge resection of the right upper lobe was performed.
Grossly, a grey-white solid mass was observed in the surgical specimen. Histologically, the mass was composed of atypical cells proliferating with tubular, cribriform and solid structures. At the margins of the lesion, tumor cells infiltrated into the alveolar septa (so-called interstitial spread), and overlying pneumocytes exhibited hyperplastic change and nuclear atypia.
Immunohistochemically, two types of cells were recognized. One was a distribution of epithelial cells showing cytokeratin (CK) AE1/AE3, CK 5/6 positivity. The other was a proliferation of cells with positive of myoepithelial markers, such as p40, p63, and α SMA. C-Myb was also partially positive in myoepithelial cells of the lesion. TTF-1 and Napsin A were positive for overlying pneumocytes, but negative for tumor cells.
On the basis of the above findings, we have made a diagnosis of pulmonary metastasis of sinonasal adenoid cystic carcinoma. When metastatic tumor cells spread within the alveolar septa and accompanied by hyperplastic change and nuclear atypia of pneumocytes, it may be difficult to distinguish from primary lung adenocarcinoma histologically. In order to diagnose correctly the tumor exhibiting interstitial spread, it is important to consider the clinical course and immunostaining findings together.

Poster 9 (P-9)

A case of adult granulosa cell tumor with sex cord tumor with annular tubules-like morphology, both of which have a common mutation of FOXL2 p.C134W.

喜多村恭平 Kyohei Kitamura, Yuki Teramoto, Naoki Goda, Hiroaki Ito, Sachiko Minamiguchi, Hironori Haga
Department of Diagnostic Pathology, Kyoto University Hospital

Adult granulosa cell tumor (AGCT) is a tumor composed of granulosa cells growing in a variety of patterns. FOXL2 C134W mutation is a characteristic mutation of AGCT[1].
Sex cord tumor with annular tubules (SCTAT) is a rare tumor, accounting for <1% of all sex cord tumors. It shows characteristic ring-like tubules with basement membrane-like materials (annular tubules). Few reports show the relationship of AGCT with SCTAT. Herein, we report a case of AGCT with SCTAT-like morphology, which has a common mutation of FOXL2 p.C134W.
The patient is a postmenopausal woman in her 60s. In a previous hospital, a 9.0 cm left ovarian tumor was found, and the patient was followed up. Six months later, she felt abdominal distention and pain. Abdominal ultrasound showed ascites and the tumor had increased to 12 cm in size. Then she was referred to Kyoto University Hospital. Blood tests showed low FSH and high estrogen (E2) levels. Based on these findings and MRI, AGCT was suspected. Total hysterectomy, bilateral salpingo-oophorectomy, partial omentectomy, and peritoneal biopsy were performed.
Grossly, the left ovarian tumor was 15.0 x 13.0 x 3.0 cm in size with a ruptured capsule. The contents were yellow to tan solid tumor with hemorrhage.
Microscopically, the tumor exhibited various growth patterns. A diffuse pattern of sheet-like growth with dilated vessels was predominant, while a trabecular pattern, microfollicular pattern, and “watered silk pattern” were observed. Tumor cells had scant cytoplasm, oval nuclei, prominent nucleoli, and coffee bean-like nuclear grooves. Call-Exner bodies were found. These findings were compatible with AGCT.
In addition, ring-like tubules with basement membrane-like materials were observed at the periphery. This was a SCTAT-like pattern. Immunohistochemically, both AGCT and SCTAT-like components were positive for FOXL2. For further investigation, we performed Sanger sequencing in both components. The result revealed both had the

same FOXL2 C134W mutation, indicating that AGCT showed SCTAT-like morphology. This is the second case of AGCT with SCTAT-like morphology, which showed their identical mutation profile[2].

1. Jamieson S, et al. The FOXL2 C134W mutation is characteristic of adult granulosa cell tumors of the ovary. Mod Pathol. 2010;23:1477-1485.
2. Chang RJ, et al. Sex Cord Tumor With Annular Tubules-Like Histologic Pattern in Adult Granulosa Cell Tumor: Case Report of a Hitherto Unreported Morphologic Variant. Int J Surg Pathol. 2021;29:433-437.

The 8th Japan-Taiwan Conjoint Slide Conference Secretariat

☆ Yuki Teramoto (web designer & booklet editor)

☆ Kaoru Ijiri (progress manager & tour coordinator)

☆ Yukako Nakajima (venue setting up & registration)

☆ All staff of the Department of Diagnostic Pathology, Kyoto University Hospital